crystals

MDPI

Article

Intermolecular Hydrogen Bonding in Alpha-Hydroxy Carboxylic Acids Crystals: Connectivity, Synthons, Supramolecular Motifs

Alexander A. Bredikhin *, Robert R. Fayzullin, Aidar T. Gubaidullin and Zemfira A. Bredikhina

Arbuzov Institute of Organic and Physical Chemistry, FRC Kazan Scientific Center of Russian Academy of Sciences, 8 Arbuzov Street, Kazan 420088, Russia
* Correspondence: baa@iopc.ru

Abstract: Synthon theory underlies the analysis and empirical prediction of the crystal structure. Supramolecular synthons (SMSs) formed by intermolecular hydrogen bonds, such as carboxylic $\mathbf{R_2^2(8)}$ and $\mathbf{C_1^1(4)}$ and alcoholic $\mathbf{C_1^1(2)}$ ones, are among the most popular. The subject of this publication is the identification of specific synthons in alpha-hydroxycarboxylic acids (AHAs) crystals, in which carboxyl and alcohol fragments are present simultaneously. A series of 11 single-enantiomeric and racemic crystals of substituted lactic acids, the simplest chiral AHA family, were prepared and studied by the single-crystal X-ray diffraction (SC-XRD) method. Advanced analysis of our own and published (Cambridge Structural Database) data on the 33 crystal structures of lactic and achiral AHAs of diverse structures revealed that their supramolecular organization differs significantly from that of simple carboxylic acids. We found that in AHA crystals, hydrogen bonds RC(O)O−H···O(H)−C(R′R″)C(O)OH (in our notation HB 12) and O=C(OH)C(R′R″)−O−H···O=C(OH)R′ (HB 23) predominate. The frequency of intermolecular hydrogen bonds is interconnected with the frequency of SMSs. Thus, the synthons mentioned above occur but do not dominate in AHA crystals. Linear synthons $\mathbf{C_2^2(6)}$**:**12/23 and cyclic synthons $\mathbf{R_2^2(10)}$**:**23/23 and $\mathbf{R_3^3(11)}$**:**12/23/23 are most often implemented. An essential role in the choice of cyclic synthons is played by the chiral characteristics of the sample.

Keywords: supramolecular interactions; hydrogen-bonded organic frameworks; lactic acids; α-hydroxycarboxylic acids; synthon; chirality

Citation: Bredikhin, A.A.; Fayzullin, R.R.; Gubaidullin, A.T.; Bredikhina, Z.A. Intermolecular Hydrogen Bonding in Alpha-Hydroxy Carboxylic Acids Crystals: Connectivity, Synthons, Supramolecular Motifs. *Crystals* **2022**, *12*, 1479. https://doi.org/10.3390/cryst12101479

Academic Editor: Sławomir Grabowski

Received: 27 September 2022
Accepted: 13 October 2022
Published: 18 October 2022

1. Introduction

One of the fundamental and practically significant problems of modern natural science is the problem of crystal structure prediction starting from the chemical diagram [1]. Despite significant achievements and optimistic prospects [2], the problem posed cannot yet be considered solved at a strict ab initio level. Because the modeling of some chemical interactions is still a matter of conjecture and debate, other approaches, such as synthon theory, have been advocated [3]. In this regard, we dedicate our work to the search for new synthons essential for the formation of the crystal structure. We also are making an attempt to expand the subject and tools of such a search.

The concept of a supramolecular synthon, i.e., a repeating stable structural unit within a supermolecule crystal, formed due to various intermolecular interactions, is central to modern crystal engineering [4]. In the general series of these stable and reproducible supramolecular ensembles, synthons formed by intermolecular hydrogen bonds dominate in the crystal structures. These include the well-documented synthons of simple carboxylic acids and alcohols, namely the $\mathbf{R_2^2(8)}$ ring and $\mathbf{C_1^1(4)}$ and $\mathbf{C_1^1(2)}$ chains (Scheme 1) [4,5].

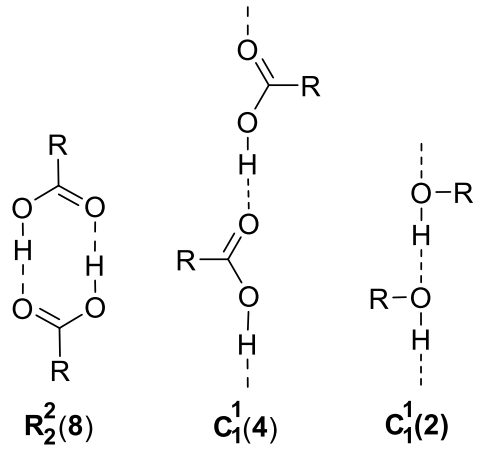

Scheme 1. Cyclic and linear synthons identified in crystals of carboxylic acids RCOOH and alcohols ROH.

Developing this topic, we asked ourselves about the synthons that are realized in the crystals of compounds, in which the carboxyl and hydroxyl functions are present in one molecule, as, for example, in the molecules of alpha-hydroxycarboxylic acids (AHAs).

The AHA family, many of whose representatives (for example, tartaric, lactic, malic, and citric acids) are of natural origin, in addition to practical relevance, has a particular interest. After all, it was tartaric and lactic acids that served as the objects of historical research by Louis Pasteur [6,7] and Johannes Wislicenus [8,9], which laid the foundations of modern stereochemistry.

The total group of α-hydroxycarboxylic acids studied by single-crystal X-ray diffraction (SC-XRD) is large and diverse enough that their structures cannot be analyzed sufficiently in one article. We limited our task, firstly, to the family of achiral AHAs, which have two identical substituents at the tetrahedral carbon atom (structure I in Scheme 2). The simplest AHA, glycolic acid (I, R=H), belongs to this family. In addition to their relative simplicity, achiral AHAs are interesting in that their crystallization is not restricted by their molecular symmetry.

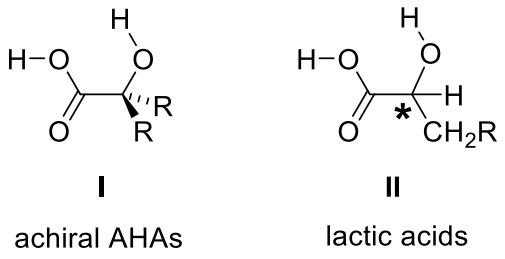

Scheme 2. Molecular structure of achiral alpha-hydroxy acids (**I**) and lactic acids (**II**). Asterisk in the diagram indicate chiral center.

However, most α-hydroxycarboxylic acids are chiral, and it is often this feature that makes them interesting for practice. Previously, using the example of a uniformly organized series of chiral compounds, we showed that the crystal packings of racemic and enantiopure crystals differ at the level of supramolecular motifs predominating in them [10,11]. In this work, we will analyze the crystal structure of lactic acids (structure II in Scheme 2). This family is presented in the literature rather modestly. This is especially true for the "racemic vs. single-enantiomeric" compound pairs. For this reason, we considered it possible to supplement the literature material with our data for 11 substituted lactic acids obtained by us and studied in this work.

In the first stage of our study, we will try to develop general methods for identifying and describing the system of intermolecular bonds in which the $R_1R_2C(OH)–C(O)OH$ frag-

ment takes part. Further, we will apply the developed methodology to the intended families and, based on the systematization of structural data, we will formulate several general features of the supramolecular organization of the crystal packing of α-hydroxycarboxylic acids.

2. Materials and Methods

2.1. Instrumentation

Melting points for general purposes were determined using a Boëtius apparatus. Optical rotations were measured on a Perkin-Elmer model 341 polarimeter (PerkinElmer, Waltham, MA, USA), and concentration *c* is given as g/100 mL.

2.2. Materials

The synthesis of the racemic and enantiopure samples of compounds **1**–**6** has been described in detail in our previous work [12]. The single crystals of the compounds *rac*-**1**–**4**, *rac*-**6**, (*S*)-**1**–**5**, and (*R*)-**6** investigated by X-ray diffraction in this paper were prepared by slow evaporation of solutions of the corresponding samples in an appropriating solvent. Characteristics of the obtained crystals agree with literature data [12] and are shown below (for each compound, the solvent or mixture of solvents in which the crystals were grown for X-ray analysis is indicated in parentheses):

rac-2-Hydroxy-3-phenoxypropanoic acid, *rac*-**1.** Mp 157–159 °C (methanol–toluene).

(*S*)-2-Hydroxy-3-phenoxypropanoic acid, (*S*)-**1.** Mp 132–134 °C (methanol), $[\alpha]_D^{20}$ +25.6 (*c* 1.2, MeOH).

rac-2-Hydroxy-3-(2-methylphenoxy)propanoic acid, *rac*-**2.** Mp 153–154 °C (methanol).

(*S*)-2-Hydroxy-3-(2-methylphenoxy)propanoic acid, (*S*)-**2.** Mp 122–124 °C (methanol), $[\alpha]_D^{20}$ +26.8 (*c* 0.7, MeOH).

rac-3-(2-Chlorophenoxy)-2-hydroxypropanoic acid, *rac*-**3.** Mp 136–137 °C (hexane–MTBE).

(*S*)-3-(2-Chlorophenoxy)-2-hydroxypropanoic acid, (*S*)-**3.** Mp 135–137 °C (toluene–MTBE), $[\alpha]_D^{20}$ +14.6 (*c* 1, MeOH).

rac-3-(2-Bromophenoxy)-2-hydroxypropanoic acid, *rac*-**4.** Mp 147–149 °C (ethyl acetate–toluene).

(*S*)-2-Hydroxy-3-(2-bromophenoxy)propanoic acid, (*S*)-**4.** Mp 127–129 °C (methanol); $[\alpha]_D^{20}$ +14.7 (*c* 1.1, MeOH).

rac-2-Hydroxy-3-(2-methoxyphenoxy)propanoic acid, *rac*-**5.** Mp 98–100 °C (methanol–toluene).

(*S*)-2-Hydroxy-3-(2-methoxyphenoxy)propanoic acid, (*S*)-**5.** Mp 70–72 °C (cyclohexane–ether), $[\alpha]_D^{20}$ +16.9 (*c* 0.9, MeOH).

rac-3-Chloro-2-hydroxypropanoic acid, *rac*-**6.** Mp 78–80 °C (chloroform).

(*R*)-3-Chloro-2-hydroxypropanoic acid, (*R*)-**6.** Mp 89–91 °C (chloroform), $[\alpha]_D^{20}$ +3.9 (*c* 9, H_2O).

2.3. Single Crystal X-ray Diffraction

The X-ray diffraction data for the single crystals *rac*-**1**–**4**, *rac*-**6**, (*S*)-**4**, and (*R*)-**6** were collected on a Bruker KAPPA APEX II CCD automated four-circle diffractometer at 100(2) K: graphite monochromator, λ(Mo *K*α) = 0.71073 Å, ω/φ-scanning with a step of 0.5°. Datasets for the single crystals of compounds (*S*)-**1**–**4** were collected on a Bruker KAPPA APEX Duo four-circle diffractometer at 120(2) K: graphite monochromator, λ(Cu *K*α) = 1.54178 Å, ω/φ- or ω-scanning with a step of 0.5°. Crystal (*S*)-**5** was studied using synchrotron radiation (λ = 0.79312 Å) at 100(2) K. Data processing was carried out using the *APEX*3 or *XDS* [13] software packages. The structures were solved by the intrinsic phasing method using *SHELXT*-2018/2 [14] and refined by full-matrix least-squares refinement on F^2 using *SHELXL*-2018/3 [15]. Non-hydrogen atoms were refined anisotropically. The positions of the hydrogen atoms of the methyl group (*rac*-**2**, (*S*)-**2**, and (*S*)-**5**) were found using a rotating group refinement with idealized tetrahedral angles. Positions of H(O) hydrogen atoms were determined from difference Fourier maps and refined isotropically. The other

hydrogen atoms were inserted at the calculated positions and refined as riding atoms. The disorder, if present, was refined using a free variable and reasonable restraints on geometry and anisotropic displacement parameters. The structure *rac*-**2** was refined as a 2-component twin against a combined set of diffraction indices: the minor domain with a fractional contribution of 0.488(3) was rotated relative to the main one by 179.9° about the reciprocal axis [1.000 −0.001 −0.080] and real axis [1.000 0.000 −0.001], the twin law was 1.000 0.000 −0.002, −0.002 −1.000 −0.001, −0.159 0.002 −1.000. All experimental crystallographic data are given in the Supplementary Materials, Tables S1 and S2.

Deposition numbers CCDC 2152210–2152218 (*rac*-**1**–**4** and (*S*)-**1**–**5**) and 2155850–2155851 (*rac*-**6** and (*R*)-**6**) contain the supplementary crystallographic data for this paper. These data are provided free of charge by the joint Cambridge Crystallographic Data Centre and Fachinformationszentrum Karlsruhe Access Structures service www.ccdc.cam.ac.uk/structures.

3. Results

3.1. Preliminary Agreements

It can be expected that, in the absence of other active functional groups, supramolecular motifs in AHA crystals will be created mainly by intermolecular hydrogen bonds between fragments of carboxyl and/or secondary hydroxyl groups. In any specific case, the hydrogen atom of the hydroxyl group (indicated by number 1 in Scheme 3) and the hydrogen atom of the *sec*-hydroxyl group (number 2 in Scheme 3) can act as hydrogen bond donors. It is natural to expect that oxygen atoms of the hydroxyl and carbonyl groups, designated by numbers 1–3 in Scheme 3, will act as intermolecular hydrogen bond acceptors.

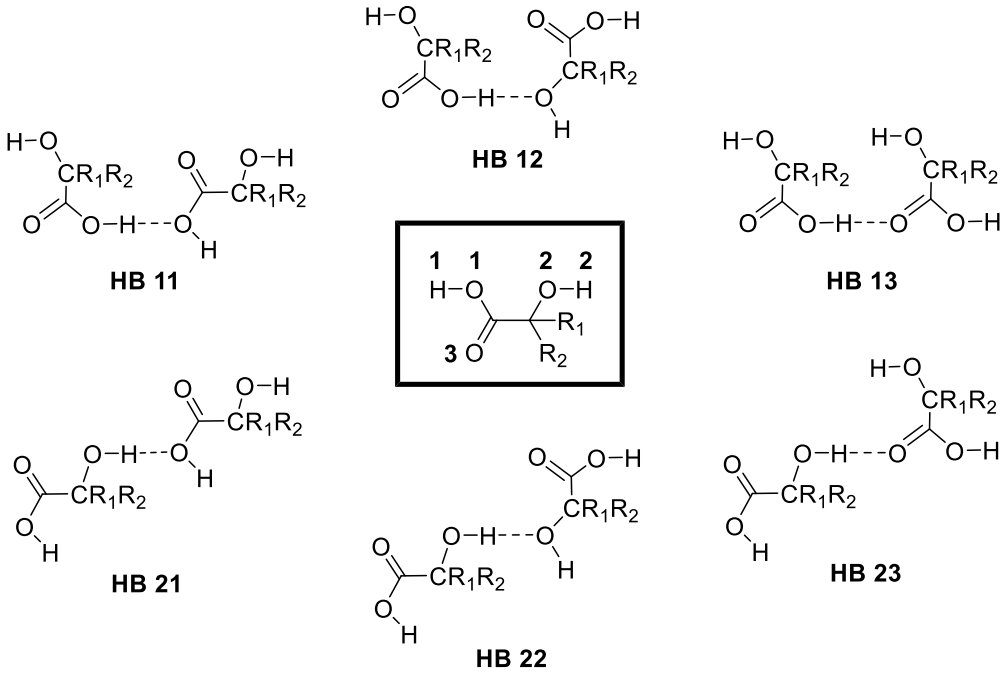

Scheme 3. Accepted numbering of donor and acceptor atoms in the α-hydroxy carboxylic acid molecule and a list of possible intermolecular hydrogen bonds (HBs) formed with their participation.

Let us make it a rule when describing a particular intermolecular hydrogen bond to mention the donor atom first and the acceptor atom second. Since donor hydrogen atoms are chemically bonded to an oxygen atom of the same number, the two-digit numbers 11, 12, 13, 21, 22, and 23 uniquely convey all possible types of individual hydrogen bonds between AHA molecules (Scheme 3).

To record regularly organized sequences of intermolecular hydrogen bonds, we will use the designations **C** (chain) and **R** (ring) introduced in [16,17], supplementing each

descriptor with a list of intermolecular hydrogen bonds forming an elementary chain link or a ring. We will separate successive hydrogen bonds with a slash. Then two synthons classical for simple carboxylic acids, 0D circle and 1D chain (Scheme 1), are designated as $\mathbf{R}_2^2$**(8):**13/13 and $\mathbf{C}_1^1$**(4):**13.

In our text, we will distinguish between the concepts of synthon ("the unit formed by synthetic operations involving intermolecular interactions" [18]) and supramolecular motif (SMM), understanding the latter as a combination of linear and/or cyclic synthons that adequately reflects the intermolecular hydrogen bond system realized in a given crystal. Other features of the notation will be explained as they become available. We begin our analysis with achiral samples.

3.2. Achiral α-Hydroxy Carboxylic Acids

A search in the Cambridge Database revealed 15 refcodes belonging to 13 molecules of individual achiral AHAs, not included in the composition of salts, solvates, etc., and also not containing in their structure the active donors and acceptors of intermolecular hydrogen bonds other than those of interest. Compounds included in the sample are listed in Table 1.

Table 1. Refcodes and chemical names of achiral α-hydroxy acids studied in this work.

N	Refcode	Name	Group, Z′	Ref.
1	NIQSUC	2,2-Dicyclopropylglycolic acid	$P\bar{1}$(2), 1	[19]
2	AFEVIR	1-Hydroxycyclopropane-1-carboxylic acid	$P2_1/c$ (14), 1	[20]
3	SIMCEX	1-Hydroxycyclohexanecarboxylic acid	$P2_1/c$ (14), 1	[21]
4	HXIBAC	2-Hydroxy-2-methylpropanoic acid	$P2_1/n$ (14), 1	[22]
5	MEWZOF	3,3,3-Trifluoro-2-hydroxy-2-trifluoromethyl)-propanoic acid	$P2_12_12_1$ (19), 1	[23]
6	TOWGEU	2-Hydroxyadamantane-2-carboxylic acid	*Pbca* (61), 1	[24]
7	HILMEV	1-Hydroxycyclobutane-1-carboxylic acid	*R*3*c* (161), 1	[25]
8	WULJAQ	2-Ethyl-2-hydroxybutanoic acid	$P\bar{1}$(2), 2	[26]
9	GLICAC01	Glycollic acid	$P2_1/c$ (14), 2	[27]
10	GLICAC10	Glycollic acid	$P2_1/c$ (14), 2	[28]
11	SOYQIG	*syn*-2-Hydroxy-2-carboxyl(4.4.1)propellane-6-ene	$C2/c$ (15), 2	[29]
12	SOYQIG01	*syn*-2-Hydroxy-2-carboxyl(4.4.1)propellane-6-ene	$C2/c$ (15), 2	[29]
13	KEYYUJ	Benzilic acid	$Pna2_1$ (33), 2	[30]
14	SILDIB	1-Hydroxycyclopentane-1-carboxylic acid	$P2_1/c$ (14), 3	[31]
15	WERHEJ	2-Hydroxy-2-propylpentanoic acid	$P2_1/c$ (14), 3	[32]

Structural formulas of molecules corresponding to refcodes are shown in Scheme 4. The order of enumeration of refcodes in the table and diagram is primarily determined by the number of symmetrically independent molecules in the unit cell of the crystal, and then by the precedence (number) of the space group.

We begin our analysis with the first item in Table 1, 2,2-dicyclopropylglycolic acid, NIQSUC. Figure 1 illustrates the system of hydrogen bonds in the crystals of this compound. As can be seen from the figure, molecules 1–4 (indicated by numbers in circles) are united by a single chain of intermolecular hydrogen bonds. In the figure, the elementary link of the chain begins with the O2−H2···O3 bond between the first and second molecules; continues with the O3–C1, C1–C2, and C2–O2 chemical bonds of the second molecule; then extends by the hydrogen bond O2−H2···O3 between the second and first molecule; goes on by the C1–O1 chemical bond in the first molecule; and ends with the O1–H1···O2 bond between the first and third molecules. Subject to the conventions adopted above, such a circuit is referred to as $\mathbf{C}_3^3$**(11):**23/23/12.

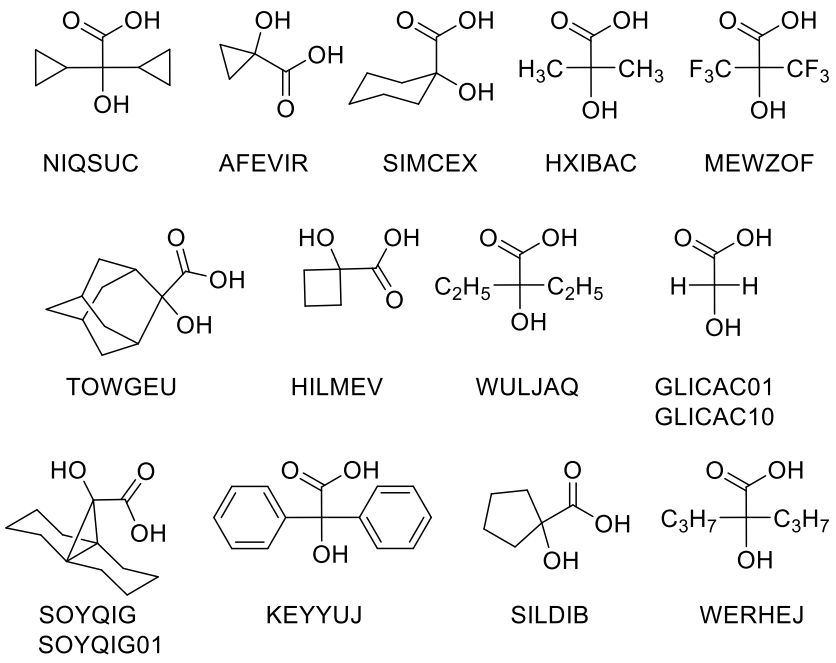

Scheme 4. Structural formulas and refcodes of selected achiral α-hydroxy carboxylic acids.

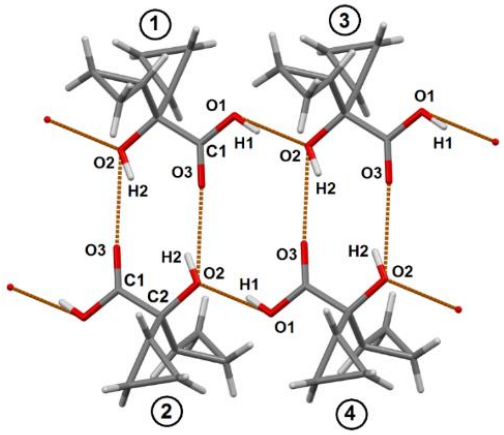

Figure 1. Fragment of the crystal packing of dicyclopropylglycolic acid NIQSUC. The numbers 1–4 in circles represent the molecules discussed in the text.

The intermolecular hydrogen bond system in the case of dicyclopropylglycolic acid presents no difficulty in interpretation. However, the regular nature of the set of identified intermolecular hydrogen bonds is often not obvious. In such cases, a useful tool for analyzing the supramolecular organization of a crystal is a connectivity diagram that explicitly reflects the sequence of bonds that form this organization. In such diagrams, we will depict chemical bonds in molecules as solid lines, and intermolecular hydrogen bonds as dashed line segments. The real linear and angular characteristics (of both the molecule and the crystal) are ignored when plotting the diagram.

For NIQSUC crystals, the diagram is shown in Scheme 5 and S1, where the chain $\mathbf{C}_3^3$**(11):**23/23/12 is shown by a broken line, and the small and large centrosymmetric cycles $\mathbf{R}_2^2$**(10):**23/23 and $\mathbf{R}_4^4$**(12):**12/23/12/23, generated by it, are marked with blue and green circles. We will make it a rule to list the chains first and the rings second when describing supramolecular motifs. In such descriptions, chains and rings are written in increasing order of the length of the elementary link of the chain or the size of the ring.

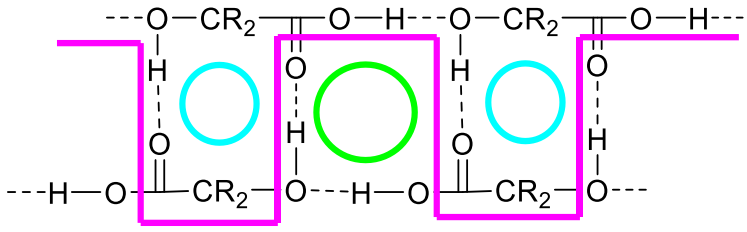

Scheme 5. Connectivity diagram in NIQSUC crystals. The purple broken line corresponds to the continuous chain $\mathbf{C_3^3(11)}$:12/23/23, the colored circles visualize the rings $\mathbf{R_2^2(10)}$:23/23 and $\mathbf{R_4^4(12)}$:12/23/12/23.

The following AFEVIR refcode in Table 1 belongs to 1-hydroxycyclopropane carboxylic acid. Its crystals (Figure 2) simultaneously contain the classical centrosymmetric dimer $\mathbf{R_2^2(8)}$:13/13 of carboxylic acids RCOOH and the $\mathbf{C_1^1(2)}$:22 chain typical of simple alcohols ROH. In this case, the chain, binding molecules 1, 2 and 3 (as well as 1′, 2′ and 3′), is formed around an open symmetry element, the screw axis 2_1.

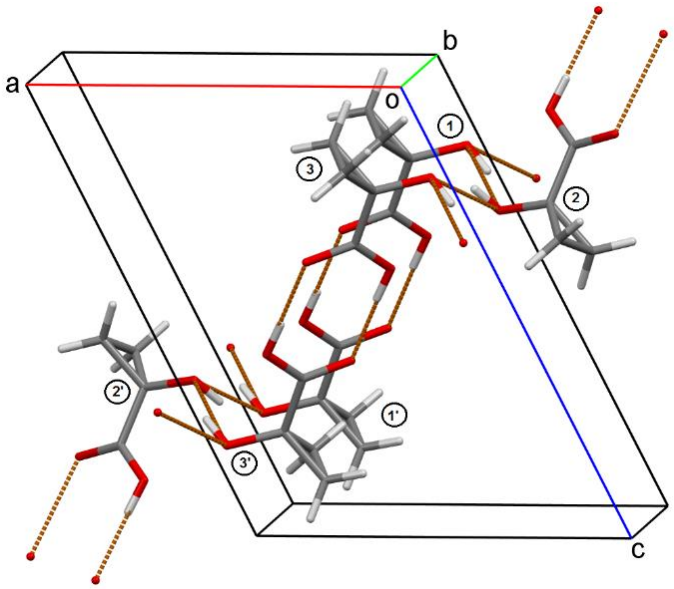

Figure 2. Fragment of the crystal packing of 1-hydroxycyclopropane carboxylic acid AFEVIR. The numbers 1–3 and 1′–3′ in circles represent the molecules discussed in the text.

If the presence of these two synthons is evident already from the figure, then the presence of the large ring $\mathbf{R_6^6(24)}$:22/22/13/22/22/13 becomes apparent only from the corresponding connectivity diagram (Scheme S2). Thus, the total supramolecular motif for this AHA is written as $\mathbf{C_1^1(2)}$:22; $\mathbf{R_2^2(8)}$:13/13;$\mathbf{R_6^6(24)}$:22/22/13/22/22/13.

The connectivity diagram for 1-hydroxycyclohexanecarboxylic acid crystals (SIMCEX) describes the SMM, which includes three synthons: $\mathbf{C_1^1(5)}$:23, $\mathbf{R_4^4(12)}$:23/12/23/12, and $\mathbf{R_4^4(20)}$:{23}{12}{23}{12} (Scheme S3). As one might expect, the endless chains $\mathbf{C_1^1(5)}$:23 marked in purple straight lines are formed around open symmetry elements, screw axes 2_1 parallel to the 0*b* direction (Figure 3). The chains are combined into a single motif due to the hydroxyl groups of carboxyl functions that are not occupied in the chains. In this case, centrosymmetric unidirectional cycles $\mathbf{R_4^4}$ **(12)**:23/12/23/12, formed with the participation of four different molecules and marked in the diagram by green circles, are clearly visible in the figure.

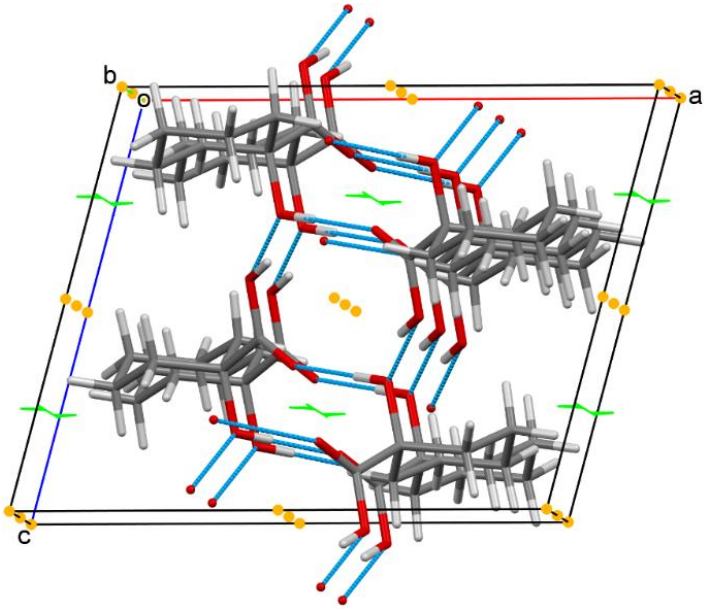

Figure 3. Fragment of the crystal packing of 1-hydroxycyclohexanecarboxylic acid SIMCEX.

The connectivity diagram (Scheme S3) also makes it possible to identify multidirectional cycles $\mathbf{R}_4^4$**(20):**{23}{12}{23}{12}, indicated by blue ovals, which are completely non-obvious from Figure 3. Let us clarify that in unidirectional cycles (and in other regularly organized intermolecular hydrogen bond sequences) sequences O−H···O . . . O−H···O . . . , i.e., "donor–acceptor . . . donor–acceptor . . . ", are always oriented uniformly. Multidirectional cycles necessarily contain oppositely directed fragments O−H···O . . . O···H−O . . . , i.e., "donor–acceptor . . . acceptor–donor". In our notation, the multidirectional intermolecular hydrogen bond sequences are enclosed in curly brackets.

The connectivity scheme (and hence the SMM) in α-hydroxyisobutyric acid (HXIBAC) crystals is the same as that in NIQSUC crystals (Scheme S1). Note that the nontrivial open symmetry elements, which are present in HXIBAC crystals, namely the glide planes and the screw axes, turn out to be unused in the construction of the SMM.

Connectivity in crystals of 3,3,3-trifluoro-2-hydroxy-2-trifluoromethyl)-propanoic acid, MEWZOF, is described by Scheme S4. Its physical implementation is shown in Figure 4. It can be seen from the figure that the donor fragment O1−H1 of the conditionally first molecule is bound to the acceptor oxygen atom O2 of the conditionally second molecule. The second molecule is bound by an O2−H2···O3 hydrogen bond with the third molecule. Molecule 3 continues the chain by bonding O1−H1···O2 with molecule 4, which forms intermolecular hydrogen bond O2−H2···O3 with molecule 2. Then the recursion is repeated, generating the chain $\mathbf{C}_2^2$**(6):**12/23, which is formed around one of the screw axes 2_1 parallel to the 0*a* direction. In Scheme S4, this circuit is indicated by a broken purple line. In its development, this chain generates secondary synthons, adjacent rings $\mathbf{R}_3^3$**(11):**12/23/23, indicated by green ellipses. The final motif is a set of linear and cyclic synthons $\mathbf{C}_2^2$**(6):**12/23; $\mathbf{R}_3^3$**(11):**12/23/23.

Figure 5 represents a fragment of the packing of molecules in 2-hydroxyadamantane-2-carboxylic acid (TOWGEU) crystals, and Scheme S5 conveys the connectivity in these crystals. It is easy to spot $\mathbf{C}_2^2$**(6):**12/23 circuits in the diagram, indicated by purple broken lines. United by the bodies of molecules (hydrocarbon fragments), these chains generate multidirectional cycles $\mathbf{R}_4^4$**(16):**{23/12/23}{12} (green ovals). The cumulative SMM corresponds to the formula $\mathbf{C}_2^2$**(6):**12/23; $\mathbf{R}_4^4$**(16):**{23/12/23}{12}.

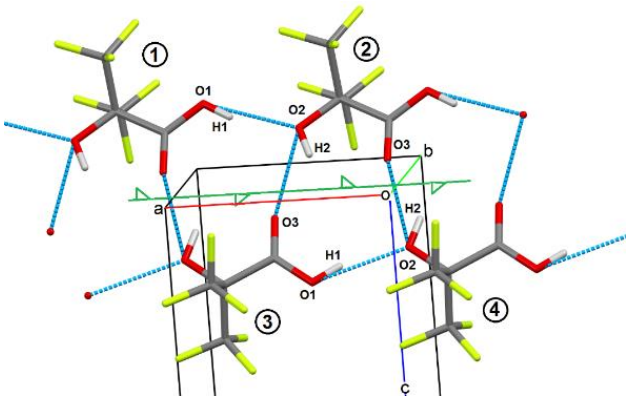

Figure 4. Fragment of the crystal packing of 3,3,3-trifluoro-2-hydroxy-2-trifluoromethyl-propanoic acid, MEWZOF. The numbers 1–4 in circles represent the molecules discussed in the text.

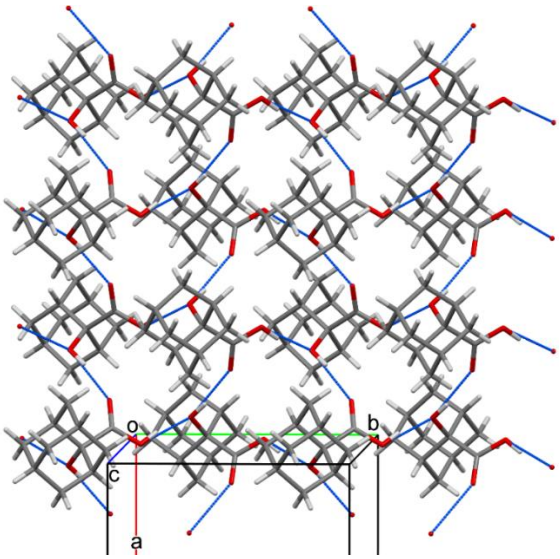

Figure 5. Fragment of the crystal packing of 2-hydroxyadamantane-2-carboxylic acid, TOWGEU.

The trigonal symmetry of HILMEV crystals makes visual analysis of the supramolecular structure difficult, but the connectivity diagram (Scheme S6) makes the task easier. It follows from the diagram that the main supramolecular synthon here is the $\mathbf{C_2^2(6)}$**:**12**/**23 chains marked with colored broken lines. In Figure 6, the molecules that form one of these chains are marked with numbers 1–6. Each molecule takes part in the chain with either carboxyl or *sec*-hydroxyl fragments. Free groups participate in other identical chains (marked in blue and red) in such a way that each molecule is a link of two chains, but none of the molecules belong to two repeating ("one-color") chains (Scheme S6).

When considering the chains along simple third-order symmetry axes, it becomes obvious that the triples of molecules, each of which is included in two adjacent chains, form symmetrical rings $\mathbf{R_3^3(15)}$**:**23/23/23, marked in the diagram by green circles. Without insisting on the completeness, we can assume that the descriptor $\mathbf{C_2^2(6)}$**:**12/23; $\mathbf{R_3^3(15)}$**:**23/23/23 reflects the most important features of SMM in HILMEV crystals.

The achiral 2-ethyl-2-hydroxybutanoic acid WULJAQ contains two independent molecules in its asymmetric unit, each of which, in principle, should be considered to be an independent structure. However, at this stage of our study, we are primarily interested in the topology of the system of intermolecular bonds in crystals, and in this sense, (minor) differences between such molecules can be ignored. In further constructions, except for specially stipulated cases, we will adhere to this point of view.

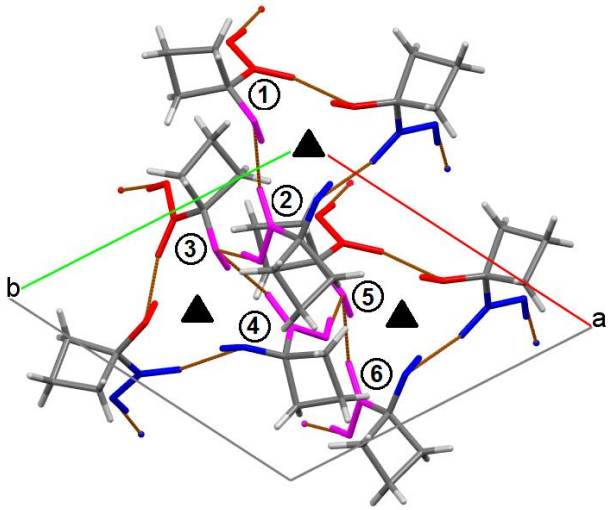

Figure 6. Fragment of the crystal packing of 1-hydroxycyclobutane-1-carboxylic acid HILMEV. The numbers 1–6 in circles represent the molecules discussed in the text.

Connectivity in WULJAQ crystals is described by the same Scheme S1 as in NIQSUC crystals. So, the same SMM $\mathbf{C}_3^3$**(11):**12/23/23; $\mathbf{R}_2^2$**(10):**23/23; $\mathbf{R}_4^4$**(12):**12/23/12/23 is realized in WULJAQ crystals. The difference between the packings is that in the previous cases, the packing is formed from equivalent molecules, and therefore both large and small rings turn out to be centrosymmetric. In this case, independent molecules alternate in the chain, so only the large ring turns out to be centrosymmetric, while the small rings adjacent to it lose their symmetry.

Refcodes GLICAC01 and GLICAC10 describe the same crystal modification of the simplest of the α-hydroxycarboxylic acids, glycolic acid. To prepare the drawings, we used cif-file GLICAC01. In glycolic acid crystals, $\mathbf{C}_1^1$**(5):**12 chains are formed along the screw axes 2_1. Being formed around a symmetry element, such columns are formed by either A or B molecules (Figure 7a). In this case, the columns are interconnected by the chain $\mathbf{C}_2^2$**(6):**12/23 (Figure 7b).

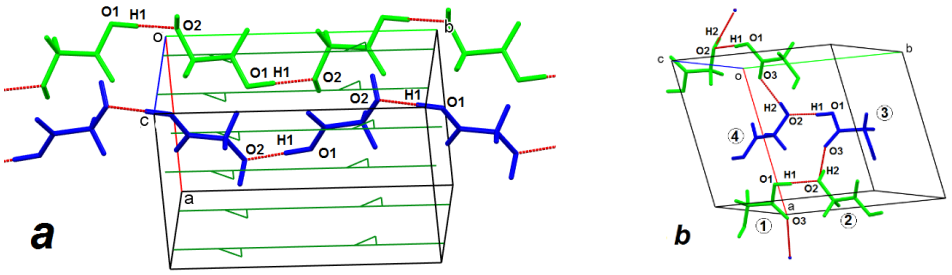

Figure 7. Fragments of the crystal packing of glycolic acid GLICAC01: (**a**) Illustrates the details of $\mathbf{C}_1^1$**(5):**12 chain formation; (**b**) illustrates the details of $\mathbf{C}_2^2$**(6):**12/23 chain formation; the numbers 1–4 denote the molecules that form a fragment of this chain.

On these grounds, it is easy to restore the connectivity in GLICAC crystals (Scheme S7), from which it becomes obvious that, along with linear synthons, the motif includes multidirectional cycles $\mathbf{R}_6^6$**(26):**{23/12/12}{12/12/23} marked with green ovals. Thus, the total supramolecular motif is described by the formula $\mathbf{C}_1^1$**(5):**12; $\mathbf{C}_2^2$**(6):**12/23; $\mathbf{R}_6^6$**(26):**{23/12/12}{12/12/23}.

Upon visual analysis of the packing in *syn*-2-hydroxy-2-carboxyl(4.4.1)propellane-6-ene SOYQIG01 crystals, the cylindrical 1D construct (Figure 8) appears to be composed solely of $\mathbf{R}_2^2$**(8):**13/13, $\mathbf{R}_4^4$**(8):**22/22/22/22, and $\mathbf{R}_4^4$**(20):**{13/22/13}{22} cycles. However, analysis of the connectivity diagram (Scheme S8) makes it possible to detect $\mathbf{C}_3^3$**(12):**22/22/13 chains penetrating and consolidating the entire crystal packing.

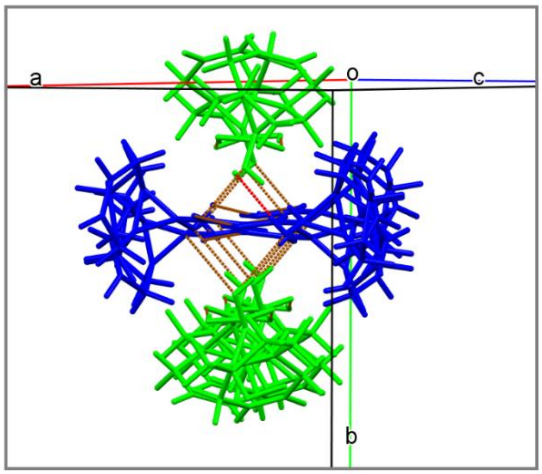

Figure 8. Fragments of the crystal packing of *syn*-2-hydroxy-2-carboxyl(4.4.1)propellane-6-ene SOYQIG_01.

In crystals of 2-hydroxy-2,2-diphenylacetic acid (benzylic acid, KEYYUJ), the motif $\mathbf{C_2^2(6)}$**:**12/23;$\mathbf{R_3^3(11)}$**:**12/23/23 already known in the example of MEWZOF (Scheme S4, Figure 9) is realized. The difference here is that in the case of MEWZOF the chain $\mathbf{C_2^2(6)}$**:**12/23 was formed around the screw axis 2_1 (Figure 4). Two independent molecules in benzylic acid crystals cannot be combined into a common synthon around the first-kind symmetry element. In this case, a single chain is formed along the second-kind symmetry element, namely the glide plane. The same way of realizing the same motif but with the participation of three independent molecules is also realized in WERHEJ crystals (Figure 10).

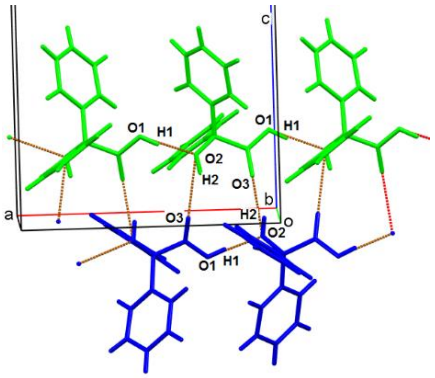

Figure 9. Fragment of the crystal packing of benzylic acid KEYYUJ.

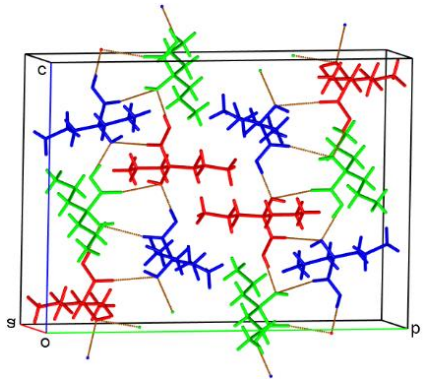

Figure 10. Fragment of the crystal packing of 2-hydroxy-2-propylpentanoic acid WERHEJ.

In 1-hydroxycyclopentane-1-carboxylic acid (SILDIB) crystals, three symmetrically independent molecules form $\mathbf{C}_1^1$ **(2):**22 chains (Figure 11). In the same figure, the cyclic "carboxylic" synthons $\mathbf{R}_2^2$**(8):**13/13 are striking. We have already seen such a combination of synthons in the example of AFEVIR crystals (Scheme S2), but in this case, symmetrically independent molecules in the crystal turn out to be topologically nonequivalent, which leads to a transformation of the connectivity scheme and, as a consequence, to the appearance of other synthons.

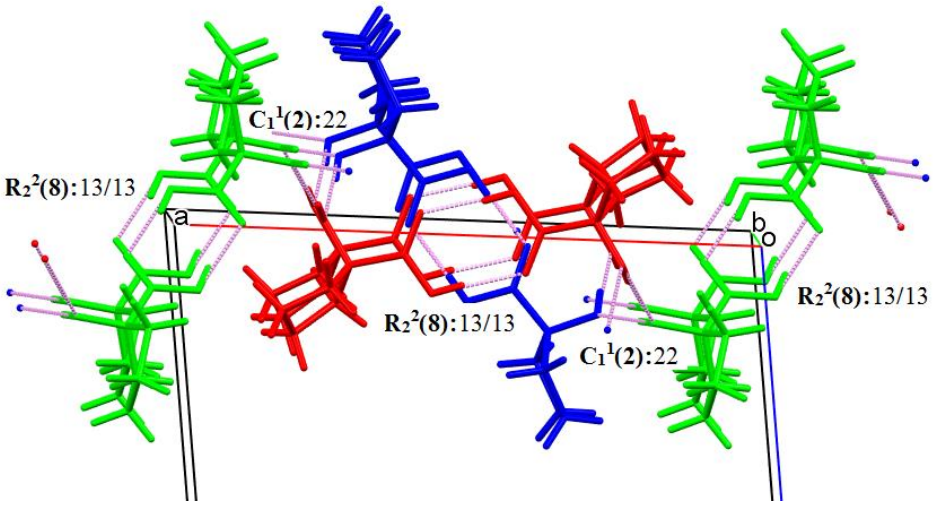

Figure 11. Fragment of the crystal packing of 1-hydroxycyclopentane-1-carboxylic acid SILDIB.

As seen in Figure 11, the $\mathbf{C}_1^1$ **(2):**22 chains are formed around the approximate triple axes parallel to the 0*b* direction, rather than around the 2_1 axes as in AFEVIR crystals (Figure 2). Carboxyl fragments of molecules do not participate in endless chains; they form $\mathbf{R}_2^2$**(8):**13/13 dimers classical for carboxylic acids. Being centrosymmetric, these rings are formed only by the same molecules AA (green), BB (blue), or CC (red). However, if the $\mathbf{R}_2^2$**(8):**13/13 rings, formed by molecules B and C, unite two $\mathbf{C}_1^1$ **(2):**22 chains shown in Figure 11, the dimers of A molecules belong to only one of these chains and one of the other two, which are incomplete in the figure.

The topological nonequivalence of molecules A on the one hand and molecules D and C on the other is clearly seen in the connectivity diagram in SILDIB crystals (Scheme S9). However, both large cycles, marked in the diagram with pink and green ovals, are formed with equal participation of all three independent molecules. As a result, SMM SILDIB is represented by four synthons $\mathbf{C}_1^1$ **(2):**22; $\mathbf{R}_2^2$**(8):**13/13; $\mathbf{R}_5^5$**(22):**22/13/22/22/13; $\mathbf{R}_8^8$**(28):**22/22/22/13/22/22/22/13.

This completes the list of 13 achiral AHAs studied in our work. In our opinion, such a sample is too small for separate statistical processing. Therefore, we further turn to the analysis of the crystal structure of lactic acids (Scheme 2).

3.3. Lactic Acids

If we do not consider cocrystals, solvates, and salts and do not include in the sample compounds with active intermolecular hydrogen bond donors and acceptors other than those of interest to us, then 12 hits corresponding to O=C(OH)–CH(OH)–CH_2R lactic acid crystals are found in the Cambridge Database. Of these, four belong to crystals of lactic acid proper and five belong to crystals of phenyl lactic acid. We added our own data for compounds **1**–**6** to the same sample. In the current year, a publication [33] that contains data on the crystal structure of chloro-, bromo-, and iodolactic acids **6**–**8** appeared. The structures of all compounds whose supramolecular organization was studied in this work are shown in Scheme 6.

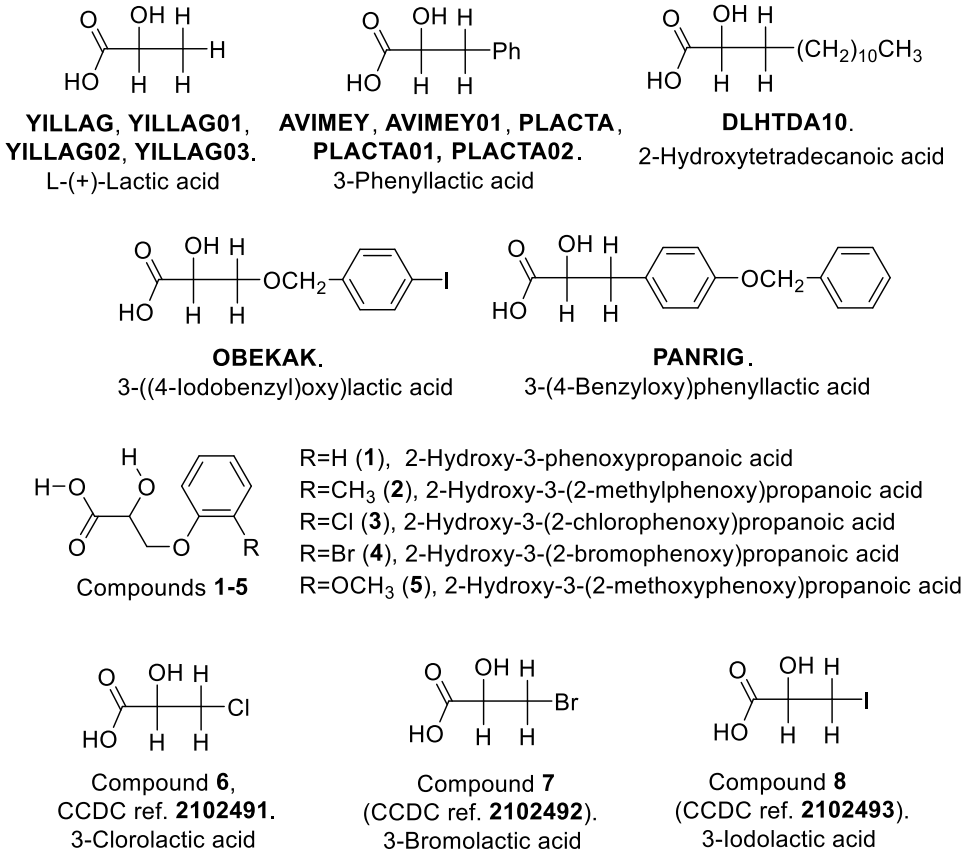

Scheme 6. Structures and chemical names of lactic acids, for which own and published crystallographic data were used in this work.

3.3.1. Racemic Lactic Acids

The first group that we consider is racemic crystals, the packing of which formally has no restrictions on symmetry. We consider our own data simultaneously with the available literature data. The total set of racemic crystalline lactic acids tested is shown in Table 2.

Table 2. Refcodes or identifiers (IDs) and chemical names of racemic lactic acids studied in this work.

N	Refcode, ID	Name	Group, Z′	Ref.
1	*rac*-DLHTDA10	*rac*-2-Hydroxytetradecanoic acid	$P\bar{1}$(2), 1	[34]
2	*rac*-1	*rac*-2-Hydroxy-3-phenoxypropanoic acid	$P2_1/c$ (14), 1	
3	*rac*-AVIMEY	*rac*-2-Hydroxy-3-phenylpropionic acid	$P2_1/c$ (14), 1	[35]
4	*rac*-8	*rac*- 3-Iodolactic acid	$P2_1/c$ (14), 1	[33]
5	*rac*-3	*rac*-3-(2-Chlorophenoxy)-2-hydroxypropanoic acid	*Pbca* (61), 1	
6	*rac*-4	*rac*-3-(2-Bromophenoxy)-2-hydroxypropanoic acid	*Pbca* (61), 1	
7	*rac*-2	*rac*-2-Hydroxy-3-(2-methylphenoxy)propanoic acid	$P2_1/c$ (14), 2	
8	*rac*-6	*rac*-3-Chlorolactic acid	$P2_1/c$ (14), 2	
9	*rac*-AVIMEY01	*rac*-3-Phenyl-lactic acid	$P2_1/c$ (14), 2	[36]
10	*rac*-7	*rac*-3-Bromolactic acid	$P2_1/c$ (14), 2	[33]

Connectivity

Connectivity in crystals of racemic 2-hydroxytetradecanoic acid DLHTDA10 is represented by Scheme S10, and the physical organization of intermolecular hydrogen bonds is depicted in Figure 12. From the scheme and figure, the presence of $\mathbf{C}_1^1$ **(5):**21 chains, rings $\mathbf{R}_2^2$**(8):**13/13 (indicated by green ellipses), and other centrosymmetric rings $\mathbf{R}_4^4$**(14):**21/13/21/13 (blue ellipses) is obvious.

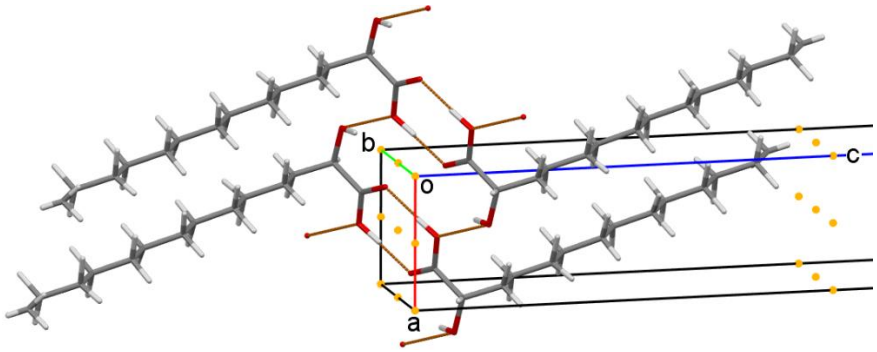

Figure 12. Physical formation of SMM in DLHTDA10 crystals.

Next on the list is 2-hydroxy-3-phenyloxypropanoic acid, *rac*-**1**. The physical organization of chains and rings in *rac*-**1** crystals is illustrated in Figure 13a, which shows that the O1–H1 hydroxyl fragment of the conditionally first molecule is hydrogen bonded to the O2 atom of the conditionally second molecule. In turn, the hydroxyl fragment O2–H2 is linked to the O3 atom of the conditionally third molecule. The active fragment closest to the O3 atom in the system of chemical bonds is the hydroxyl group O1–H1. The sequence {−O1−H1···O2−H2···O3−C−} is iteratively repeated, generating a helical chain $\mathbf{C_2^2(6)}$:12/23 organized along the screw axis 2_1. To form the chain, molecules 1 and 3 provide their carboxyl fragments, and molecules 2 and 4 provide their *sec*-hydroxyl groups. Fragments not occupied in this chain are involved in exactly the same adjacent chains, physically separated by fragments of the molecules participating in them (Figure 13b).

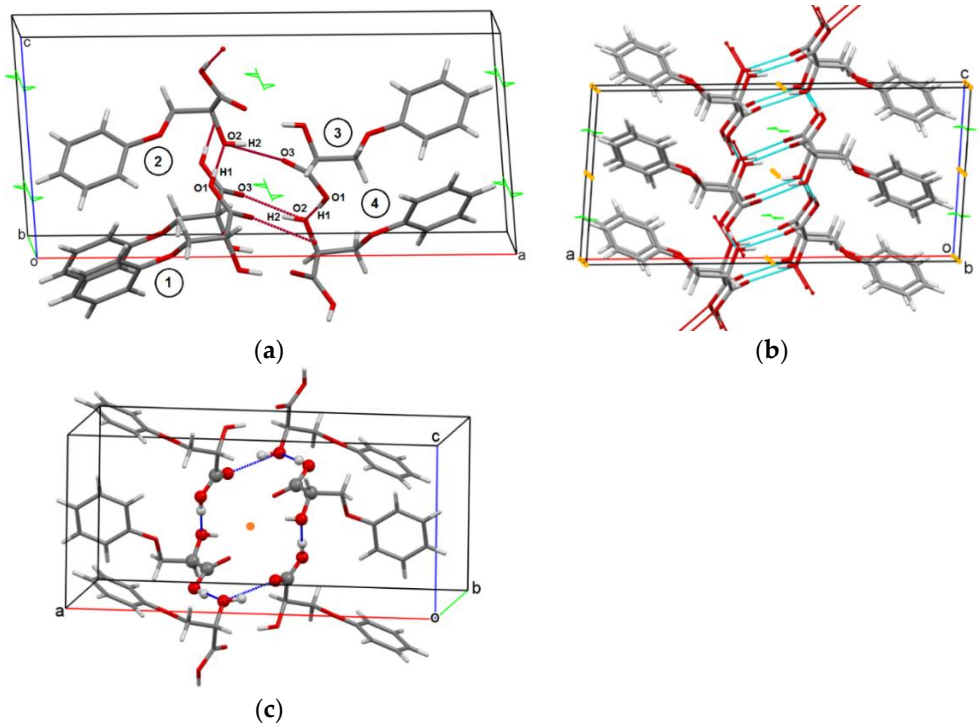

Figure 13. Intermolecular hydrogen bonding in *rac*-**1** crystals. Formation of synthons $\mathbf{C_2^2(6)}$:12/23 (**a**), $\mathbf{R_2^2(10)}$:23/23 (**b**), and $\mathbf{R_6^6(22)}$:12/23/12/12/23/12 (**c**). The numbers 1–4 in circles represent the molecules discussed in the text.

The connectivity of the *rac*-**1** crystal packing is shown in full in Scheme S11, in which chains $\mathbf{C_2^2(6)}$:12/23 are underlined in purple, and cyclic routes $\mathbf{R_2^2(10)}$:23/23 and $\mathbf{R_6^6(22)}$:12/23/12/12/23/12 indicated by green and blue ellipses, respectively. If the rings $\mathbf{R_2^2(10)}$:23/23 are easy to detect at the stage of visual analysis of the packing, then the pres-

ence of 22-term cyclic routes (Figure 13c), revealed during the analysis of the connectivity diagram, is far from obvious. Exactly the same supramolecular organization appears to be inherent in *rac*-AVIMEY crystals.

In crystals of *rac*-3-iodolactic acid *rac*-**8** (CCDC ref. 2102493), the motif $\mathbf{C}_1^1$ **(5):**23; $\mathbf{R}_4^4$**(12):**12/23/12/23; $\mathbf{R}_4^4$**(20):**{23}{12}{23}{12} is identified. This motif is already known to us from the example of the achiral acid SIMCEX (Scheme S3).

Chloro- and bromophenoxy substituted lactic acids *rac*-**3** and *rac*-**4** crystallize with a single symmetry-independent molecule in the unit cell. The connectivity diagrams turn out to be identical for both crystals and coincide in detail with the diagram in Scheme S11. The essential, but not affecting the connectivity, difference between the packings for *rac*-**3** and *rac*-**4** is that in this case the infinite chains $\mathbf{C}_2^2$**(6):**12/23 develop along the glide planes *b*, and not along the screw axes 2_1, as in the case of *rac*-**1**. The set of synthons formed in this way is again described by the sequence $\mathbf{C}_2^2$**(6):**12/23; $\mathbf{R}_2^2$**(10):**23/23; $\mathbf{R}_6^6$**(22):**12/23/12/12/23/12.

The representatives of racemic lactic acids remaining in Table 2 contain two independent molecules in the asymmetric unit. The first such example is racemic 2-hydroxy-3-(2-methylphenoxy)propanoic acid *rac*-**2**, in the crystals of which the SMM again coincides with that shown in Scheme S11. Naturally, in this case, the independent molecules that form the chains are translated along the glide planes separately.

The two samples studied, *rac*-3-chlorolactic acid *rac*-**6** and *rac*-3-bromolactic acid *rac*-**7** (CCDC ref. 2102492), crystallize in the $P2_1/c$ (14) group. We will analyze their packings, which match the details, using the example of *rac*-**6**. The packings are permeated with bi- and trifurcate intermolecular hydrogen bonds, which greatly complicates the analysis. However, if one looks along the 0*c* axis (Figure 14a), it becomes obvious that the packing is based on one-dimensional columns formed along the glide planes *c* and, therefore, consisting of either A or B molecules. Viewed from a different angle (Figure 14b), these chains represent the classic $\mathbf{C}_1^1$ **(4):**13 synthon-catemer (Scheme 1). Using the terminology of [37], such an intermolecular hydrogen bond sequence can be considered as a "structure directive" one, and all others, even those with better geometric characteristics, can be considered as "supportive" interactions.

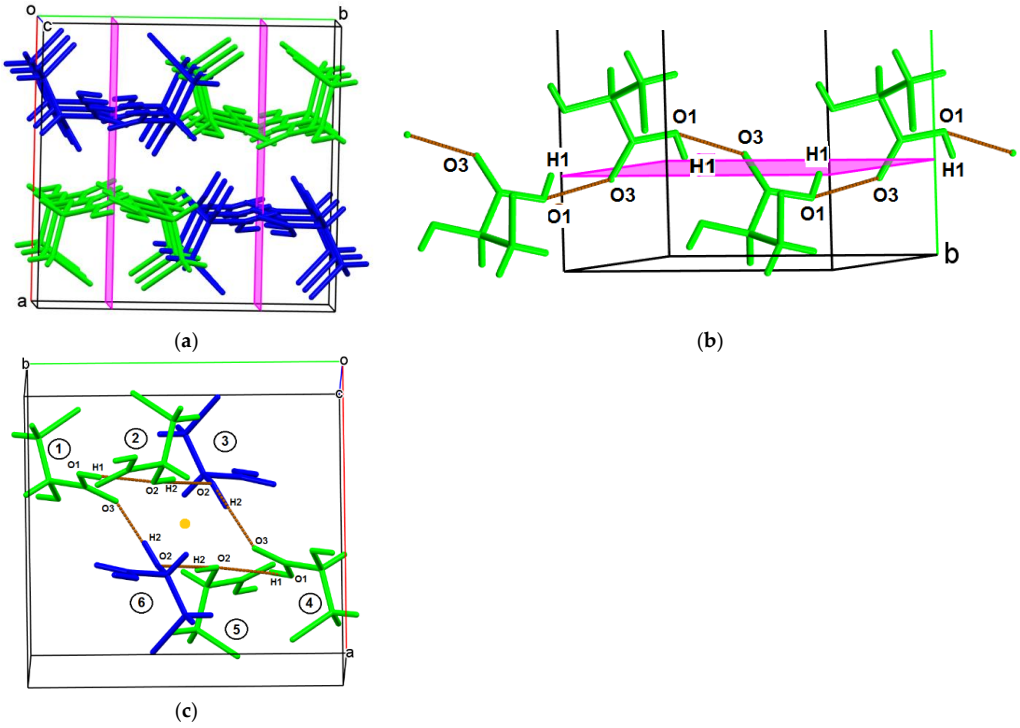

Figure 14. Packing fragments in crystals of racemic chlorolactic acid *rac*-**6**. Explanations in the text.

In the complex interweaving of intermolecular hydrogen bonds, among more or less extended associates, it is possible to distinguish a centrosymmetric closed ring $\mathbf{R}_6^6$**(16):**12/22/23/12/22/23 with a unidirectional intermolecular hydrogen bond system (Figure 14c). The ring shown in the figure consists of four A molecules and two B molecules, where the first, fifth, and sixth molecules have the *S*-configuration and the second, third, and fourth molecules have the *R*-configuration. It is clear that other rings will have different combinations and different characteristics of independent molecules. Together, with sufficient rigor for classification purposes, the SMM in *rac*-**6** (and *rac*-**7**) crystals can be characterized by the sequence $\mathbf{C}_1^1$ **(4):**13; $\mathbf{R}_6^6$**(16):**12/22/23/12/22/23.

The physical organization of intermolecular hydrogen bonds in crystals of the last representative of racemic lactic acids, *rac*-AVIMEY01, is shown in Figure 15, and the connectivity diagram is shown in Scheme S12. In the latter, chains $\mathbf{C}_1^1$**(5):**12 (purple straight lines) and $\mathbf{C}_3^3$**(11):**12/23/23 (red broken line) and cycles $\mathbf{R}_2^2$**(10):**23/23 (green ovals) and $\mathbf{R}_4^4$**(12):**12/23/12/23 (blue ovals) are easily detected.

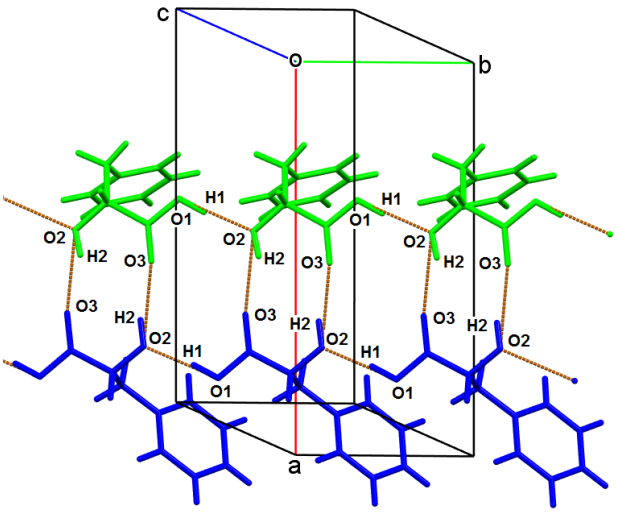

Figure 15. Physical formation of SMM in *rac*-AVIMEY01 crystals.

3.3.2. Single-Enantiomeric Lactic Acids

The last group of AHAs that we consider is single-enantiomeric samples of lactic acids, the crystal packing of which can only be realized in one of Leonhard Sohncke's 65 space groups. The total set of single-enantiomeric crystalline lactic acids studied is shown in Table 3. The structures of the studied compounds are shown in Scheme 6.

Table 3. Refcodes or identifiers (IDs) and chemical names of single-enantiomeric lactic acids studied in this work.

N	Refcode, ID	Name	Group, Z'	Ref.
1	(*S*)-1	(*S*)-2-Hydroxy-3-phenoxypropanoic acid	$P2_1$ (4), 1	
2	(*S*)-PANRIG	(*S*)-3-(4-Benzyloxy)phenyllactic acid	$P2_1$ (4), 1	[38]
3	(*R*)-6	(*R*)-3-Chlorolactic acid	$C2$ (5), 1	
4	(*S*)-3	(*S*)-3-(2-Chlorophenoxy)-2-hydroxypropanoic acid	$P2_12_12_1$ (19), 1	
5	(*S*)-4	(*S*)-3-(2-Chlorophenoxy)-2-hydroxypropanoic acid	$P2_12_12_1$ (19), 1	
6	(*S*)-5	(*S*)-2-Hydroxy-3-(2-methoxyphenoxy)propanoic acid	$P2_12_12_1$ (19), 1	
7	(*S*)-OBEKAK	(*S*)-3-((4-Iodobenzyl)oxy)lactic acid	$P2_12_12_1$ (19), 1	[39]
8	(*S*)-PLACTA01	(*S*)-3-Phenyllactic acid	$P2_12_12_1$ (19), 1	[35]
9	(*S*)-YILLAG	(*S*)-Lactic acid	$P2_12_12_1$ (19), 1	[40]
10	(*S*)-2	(*S*)-2-Hydroxy-3-(2-methylphenoxy)propanoic acid	$P2_12_12_1$ (19), 3	

First in Table 3 is (*S*)-2-hydroxy-3-phenyloxypropanoic acid, (*S*)-**1**. Figure 16 shows that the synthon-catemer $\mathbf{C}_1^1$ **(4):**13 (Scheme 1) is folded around a single symmetry element, the screw axis 2_1. The *sec*-hydroxyl group, which is not involved in the construction of the main chain, is involved as a supporting element in the intermolecular hydrogen bond with the oxygen atom of the hydroxyl groups of the carboxyl fragment, generating the cycle $\mathbf{R}_3^3$**(11):**13/13/21. The overall motif $\mathbf{C}_1^1$ **(4):**13; $\mathbf{R}_3^3$**(11):**13/13/21 is described by a simple connectivity diagram (Scheme S13).

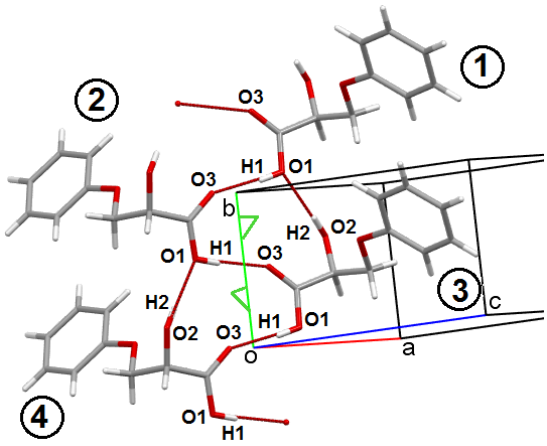

Figure 16. Physical formation of SMM in (*S*)-**1** crystals. The numbers 1–4 in circles represent the molecules discussed in the text.

Features of the crystal structure of (*S*)-3-(4-benzyloxy)phenyllactic acid, (*S*)-PANRIG, are illustrated in Figure 17. It can be seen from the figure that conditionally the first molecule (molecular numbers are enclosed in circles) is linked by an intermolecular hydrogen bond 12 to the conditionally second molecule, which forms a bond 23 to the third one. Molecule 3 forms bond 12 with molecule 4, which, in turn, forms bond 23 with the second molecule. Thus, along the screw axis 2_1, parallel to the 0*b* direction, a single chain $\mathbf{C}_2^2$**(6):**12/23 is formed. The features of connectivity in (*S*)-PANRIG crystals are more fully reflected in Scheme S4, which was encountered in the section of achiral AHAs. In this case, the SMM is the set $\mathbf{C}_2^2$**(6):**12/23;$\mathbf{R}_3^3$**(11):**12/23/23. The same connectivity scheme, and hence the same SMM, is realized in (*R*)-**6**, (*S*)-OBEKAK, and (*S*)-PLACTA01 crystals, except that the screw axis 2_1, in contrast to (*S*)-PANRIG, in these cases turns out to be parallel to the 0*a* direction.

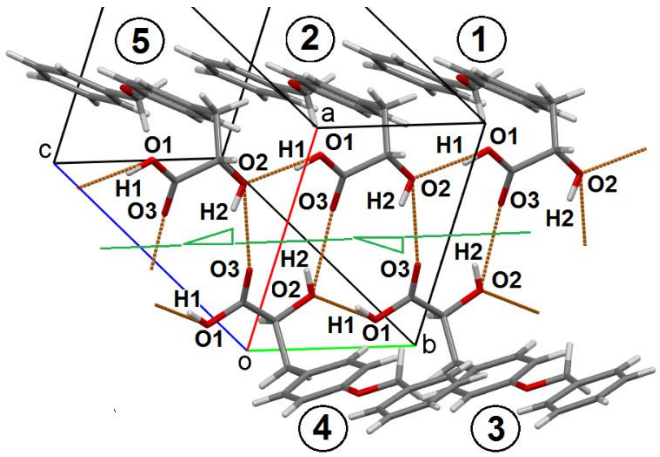

Figure 17. Physical formation of SMM in (*S*)-PANRIG crystals. The numbers 1–5 in circles represent the molecules discussed in the text.

The same intermolecular hydrogen bond system is formed in the crystals (*S*)-**3** and (*S*)-**5** (Scheme S14). Figure 18, using (*S*)-**3** crystals as an example, illustrates the physical

formation of $\mathbf{C_2^2(6)}$:12/23 chains along screw axes 2_1 parallel to the 0*b* direction (in Scheme S14 they are indicated by broken purple lines), and $\mathbf{R_4^4(16)}$ rings marked by green ovals. The final SMM can be designated as $\mathbf{C_2^2(6)}$:12/23; $\mathbf{R_4^4(16)}$:{12/23/12}{23}.

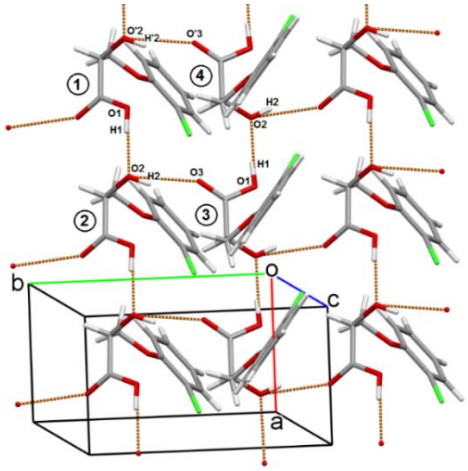

Figure 18. Physical formation of SMM in (*S*)-**3** crystals. The numbers 1–4 in circles represent the molecules discussed in the text.

Connectivity in (*S*)-**4** crystals is shown in Scheme S15, where $\mathbf{C_1^1}$ **(4):**13 chains are shown as purple broken lines and $\mathbf{C_1^1}$ **(5):**23 chains as blue straight lines. Figure 19 shows the physical arrangement of the identified synthons that collectively form the SMM $\mathbf{C_1^1}$ **(4):**13; $\mathbf{C_1^1}$ **(5):**23; $\mathbf{R_4^4(16)}$:{13/23/13}{23}.

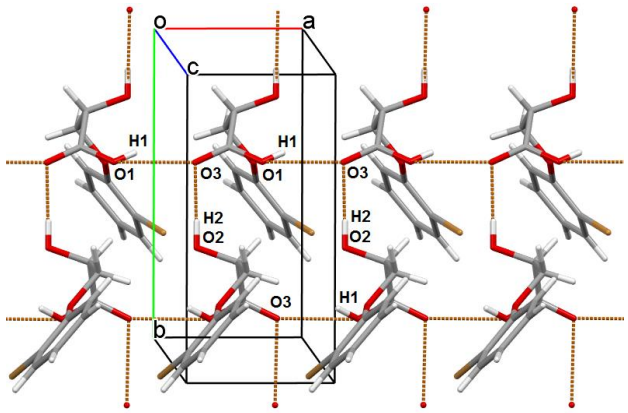

Figure 19. Physical formation of SMM in (*S*)-**4** crystals.

In crystals of unsubstituted lactic acid (*S*)-YILLAG, endless chains are formed around axes 2_1. In this case, different chains are formed around mutually orthogonal helical axes. Obviously, the complete connectivity graph in non-racemic lactic acid crystals is nonplanar, and Schemes S16 and S17 show its planar subgraphs. It follows from Scheme S16 that chains $\mathbf{C_2^2(6)}$:12/23 are formed along the 0*b* direction. During the formation of these chains, each of the contributor molecules provides either carboxyl or *sec*-hydroxyl functions to this chain. Then, unlike all previously analyzed options, each of the active groups of the molecule not included in this chain takes part in the creation of one of the four adjacent chains. Since adjacent chains in pairs, with a period of four units, turn out to be connected by the bodies of molecules entering these chains simultaneously, unidirectional 28-membered cycles arise in the intermolecular hydrogen bond system. At the same time, in (*S*)-YILLAG crystals around the 2_1 axes parallel to the 0*a* direction, $\mathbf{C_1^1}$ **(6):**23 chains are formed, which are no longer interconnected by molecular bodies but by intermolecular hydrogen bond 12. This leads to the formation of multidirectional rings $\mathbf{R_6^6(26)}$:{12/23/23}{23/23/12} (Scheme S17).

The cumulative motif can be designated by the sequence of synthons $\mathbf{C}_1^1$ **(6):**23; $\mathbf{C}_2^2$**(6):**12/23; $\mathbf{R}_6^6$**(26):**{12/23/23}{23/23/12}; $\mathbf{R}_8^8$**(28):**(12/23/12/23/12/23/12/23).

Our set is completed by (*S*)-2-hydroxy-3-(*o*-tolyloxy)propanoic acid, (*S*)-**2**, which crystallizes in the $P2_12_12_1$ (19) group with three molecules per asymmetric unit ($Z = 12$, $Z' = 3$). The connectivity scheme for this case turns out to be cumbersome (after all, there are three independent molecules) but quite intelligible (Scheme S18). Disregarding the differences between independent molecules, one can describe the SMM in (*S*)-**2** crystals as a set of three chains $\mathbf{C}_1^1$ **(5):**12, $\mathbf{C}_1^1$ **(5):**21, and $\mathbf{C}_6^6$**(14):**21/12/21/13/12/22 and three multidirectional rings $\mathbf{R}_4^4$**(14):**{21/12}{12/21}, $\mathbf{R}_4^4$**(16):**{21/13/12}{13}, and $\mathbf{R}_4^4$**(14):**{22}{12/22/12}.

4. Discussion

Table 4 lists all the supramolecular motifs identified by us in the previous section in crystals of achiral α-hydroxy carboxylic acids (whose refcodes do not have a prefix) and racemic (having the prefix *rac*-) and single-enantiomeric (having the prefixes (*S*)- or (*R*)-) lactic acids. The order of enumeration is determined primarily by the length of the elementary link of the chains involved in the construction of the SMM. Shorter chains appear first in the list. The ring components of the motif are also listed in increasing order of the size of the rings.

Table 4. Supramolecular motifs identified in the studied families of α-hydroxy carboxylic acids.

N	SMM	Representative IDs
1	$\mathbf{C}_1^1$ (2):22; $\mathbf{R}_2^2$(8):13/13; $\mathbf{R}_6^6$(24):22/22/13/22/22/13	AFEVIR
2	$\mathbf{C}_1^1$ (2):22; $\mathbf{R}_2^2$(8):13/13; $\mathbf{R}_5^5$(22):22/13/22/22/13; $\mathbf{R}_8^8$(28):22/22/22/13/22/22/22/13	SILDIB
3	$\mathbf{C}_1^1$ (4):13; $\mathbf{R}_3^3$(11):13/13/21	(*S*)-1
4	$\mathbf{C}_1^1$ (4):13; $\mathbf{R}_6^6$(16):12/22/23/12/22/23	*rac*-6, *rac*-7
5	$\mathbf{C}_1^1$ (4):13; $\mathbf{C}_1^1$ (5):23; $\mathbf{R}_4^4$(16):{13/23/13}{23}	(*S*)-4
6	$\mathbf{C}_1^1$ (5):12; $\mathbf{C}_2^2$(6):12/23; $\mathbf{R}_4^4$(16):{23/12/23}{12}	TOWGEU
7	$\mathbf{C}_1^1$ (5):12; $\mathbf{C}_3^3$(11):12/23/23; $\mathbf{R}_2^2$(10):23/23; $\mathbf{R}_4^4$(12):12/23/12/23	*rac*-AVIMEY01
8	$\mathbf{C}_1^1$ (5):12; $\mathbf{C}_1^1$ (5):21; $\mathbf{C}_6^6$(14):21/12/21/13/12/22; $\mathbf{R}_4^4$(14):{21/12}{12/21}; $\mathbf{R}_4^4$(14):{22}{12/22/12}; $\mathbf{R}_4^4$(16):{21/13/12}{13}	(*S*)-2
9	$\mathbf{C}_1^1$ (5):12; $\mathbf{C}_2^2$(6):12/23; $\mathbf{R}_6^6$(26):{23/12/12}{12/12/23}	GLICAC01
10	$\mathbf{C}_1^1$ (5):21; $\mathbf{R}_2^2$(8):13/13; $\mathbf{R}_4^4$(14):21/13/21/13	*rac*-DLHTDA10
11	$\mathbf{C}_1^1$ (5):23; $\mathbf{R}_4^4$(12):12/23/12/23; $\mathbf{R}_4^4$(20):{23}{12}{23}{12}	SIMCEX, *rac*-8
12	$\mathbf{C}_1^1$ (6):23; $\mathbf{C}_2^2$(6):12/23; $\mathbf{R}_6^6$(26):{12/23/23}{23/23/12}; $\mathbf{R}_8^8$(28):(12/23/12/23/12/23/12/23)	(*S*)-YILLAG
13	$\mathbf{C}_2^2$(6):12/23; $\mathbf{R}_2^2$(10):23/23; $\mathbf{R}_6^6$(22):12/23/12/12/23/12	*rac*-1, *rac*-AVIMEY,*rac*-2, *rac*-3, *rac*-4
14	$\mathbf{C}_2^2$(6):12/23; $\mathbf{R}_3^3$(11):12/23/23	MEWZOF, KEYYUJ, WERHEJ, (*S*)-PANRIG, (*R*)-6, (*S*)-OBEKAK, (*S*)-PLACTA01
15	$\mathbf{C}_2^2$(6):12/23; $\mathbf{R}_3^3$(15):23/23/23	HILMEV
16	$\mathbf{C}_2^2$(6):12/23; $\mathbf{R}_4^4$(16):{12/23/12}{23}	(*S*)-3, (*S*)-5
17	$\mathbf{C}_3^3$(11):23/23/12; $\mathbf{R}_2^2$(10):23/23; $\mathbf{R}_4^4$(12):12/23/12/23	NIQSUC, WULJAQ, HXIBAC
18	$\mathbf{C}_3^3$(12):22/22/13; $\mathbf{R}_2^2$(8):13/13; $\mathbf{R}_4^4$(8):22/22/22/22; $\mathbf{R}_4^4$(20):{13/22/13}{22}	SOYQIG01

As follows from Table 4, 18 different supramolecular motifs were identified in the crystal packings of 33 studied compounds, 12 of which are represented by a single example. Two motifs (lines 4 and 16) are represented by pairs of structurally very similar compounds (*rac*-**6** and *rac*-**7**; (*S*)-**3** and (*S*)-**5**). One motif (line 17) characterizes the crystallization of three achiral hydroxy acids. Only two motifs (lines 13 and 14) are inhabited by groups that are more diverse in molecular structure and larger in the number of representatives. The first of these most populated motifs is represented by racemic AHAs, and the second by achiral or enantiopure AHAs. Although the sample studied by us is relatively small, we would venture to suggest that common motifs represented simultaneously by racemic and single-enantiomeric AHAs are unlikely to be found.

First of all, we will analyze the frequency of the types of intermolecular hydrogen bonds that occur in the studied AHA crystals. Recall that the designations of intermolecular hydrogen bonds in crystals of α-hydroxycarboxylic acids are detailed in Section 3.1 and illustrated in Scheme 3. The data in Table 4 will serve as the basis for the quantitative accounting of this value in one or another set of crystals. So, for example, in the description of SMM, which is realized in AFEVIR crystals (Table 4, N1), hydrogen bond 11 never occurs; the same applies to hydrogen bonds 12, 21, and 23. Hydrogen bond descriptors 13 and 22 occur four and five times, respectively, in the description of this supramolecular motif. Table 5 summarizes the data for all AHA crystals considered in our work.

Table 5. Quantitative distribution of types of intermolecular hydrogen bonds (HBs) that form packings in 33 α-hydroxycarboxylic acid crystals studied in this work.

HB Type	Synthon Type		
	Chains	**Rings**	**Both**
11	0	0	0
12	26	70	96
13	6	18	24
21	4	6	10
22	5	26	31
23	30	79	109

First of all, the data in Table 5, as expected, demonstrate the approximate homogeneity of the distribution of intermolecular hydrogen bond types between chains and rings. It also follows from the table that the oxygen atom of the hydroxyl group of the carboxyl fragment of AHA very rarely acts as an intermolecular hydrogen bond acceptor, while the oxygen atom of the *sec*-hydroxyl group is an active acceptor and is almost as good as carbonyl oxygen in this role. Finally, two intermolecular hydrogen bonds, between the hydroxyl of the carboxyl group and the oxygen atom of the *sec*-hydroxyl group (12) and between the hydroxyl of the *sec*-hydroxyl group and the carbonyl group (23), firstly, occur equally often and, secondly, in combination make up more than 75% of all recorded intermolecular hydrogen bonds in AHA crystals.

It is interesting to compare the frequency of intermolecular hydrogen bonds between individual groups of AHAs. Table 6 compares such data for racemic and enantiopure chiral lactic acids. The table shows that the frequency distributions of hydrogen bond types in the sets practically coincide with each other, and the overall distribution for chiral acids as a whole differs little from that for the entire sample under study (Table 5).

Table 6. Frequency of intermolecular hydrogen bonds (HBs) in crystals of racemic and single-enantiomeric lactic acids.

HB Type	Racemic LA			Single-Enantiomeric LA			Both Types of LA		
	Chains	Rings	Both	Chains	Rings	Both	Chains	Rings	Both
11	0	0	0	0	0	0	0	0	0
12	7	30	37	10	19	29	17	49	66
13	2	4	6	3	6	9	5	10	15
21	1	2	3	3	4	7	4	6	10
22	0	4	4	1	2	3	1	6	7
23	8	30	38	9	22	31	17	52	69

However, the frequency ratio for individual types of intermolecular hydrogen bonds of interest to us in the family of achiral acids (Table 7) differs markedly from that in chiral acids (Table 6). It follows from Table 7 that, in addition to the hydrogen bond 11, the hydrogen bond 21 is forbidden (or at least rare) in this family. On the other hand, in this family, at least for cyclic synthons, the occurrence of hydrogen bonds between the hydroxyl groups of the sec-hydroxyl fragments noticeably increases. Obviously, this phenomenon is associated precisely with achirality, that is, with the local mirror symmetry of the fragment containing the secondary hydroxyl, which makes the latter equally accessible from both sides.

Table 7. Frequency of intermolecular hydrogen bonds (HBs) in the studied crystals of achiral α-hydroxycarboxylic acids.

HB Type	Achiral AHA		
	Chains	Rings	Both
11	0	0	0
12	11	19	30
13	1	8	9
21	0	0	0
22	4	20	24
23	13	27	40

At the end of this section, let us turn to the statistics of synthons that form AHA crystals. According to Table 4, most of the identified synthons appear to be unique or rare and are described in one or two crystals. Of the linear synthons, the $\mathbf{C}_1^1$ **(5):**23 chain occurs in 3 of the 33 crystals studied, the $\mathbf{C}_1^1$ **(4):**13 and $\mathbf{C}_1^1$ **(5):**12 chains in 4 crystals, and the $\mathbf{C}_2^2$**(6):**12/23 chain in 18 crystals. That is, intermolecular hydrogen bonds 12 and 23 prevailing in the general set are found in three of the four leading linear synthons. At the same time, the chain $\mathbf{C}_2^2$**(6):**12/23, which is formed by both of these bonds at the same time, is the absolute leader in terms of prevalence.

From the numerous and diverse family of cyclic synthons, the ring $\mathbf{R}_4^4$**(16):**{23/12/23}{12} is present in three different crystals, the ring $\mathbf{R}_2^2$**(8):**13/13 is present in four different crystals, the ring $\mathbf{R}_6^6$**(22):**12/23/12/12/23/12 is present in five different crystals, the ring $\mathbf{R}_4^4$**(12):**12/23/12/23 is present in six different crystals, the ring $\mathbf{R}_3^3$**(11):**12/23/23 is present in seven different crystals, and the ring is $\mathbf{R}_2^2$**(10):**23/23 is involved in the formation of nine crystals. Again, except for the ring $\mathbf{R}_2^2$**(8):**13/13, the most popular cyclic structures are built on the basis of intermolecular hydrogen bond 23 (the most frequent ring is $\mathbf{R}_2^2$**(10):**23/23) or combinations of intermolecular hydrogen bonds 12 and 23 in different sequences.

5. Conclusions

As expected, an increase in the number of functions capable of forming intermolecular hydrogen bonds in the case of α-hydroxycarboxylic acids leads to a complication of supramolecular motifs and an increase in the number of synthons that create these motifs. The hierarchy of synthons also changes, which is expressed in the frequency of occurrence in crystal packings. Of course, synthons classical for carboxylic acids and alcohols (Scheme 1) have not disappeared. Thus, the first synthon, in our notation $\mathbf{R_2^2(8)}$**:**13/13, is realized in AFEVIR (Figure 2), SILDIB (Figure 11), *rac*-DLHTDA10 (Figure 12), and SOYQIG01 (Figure 8) crystals. It is curious that the "alcoholic" synthon, designated $\mathbf{C_1^1}$ **(2):**22, in the set we studied, is realized only in combination with the cyclic "carboxyl" synthon in AFEVIR and SILDIB crystals. Finally, the $\mathbf{C_1^1}$ **(4):**13 chain appears in (*S*)-**1** (Figure 16), *rac*-**6** and *rac*-**7** (Figure 14b), and (*S*)-**4** (Figure 19) crystals. However, these synthons themselves, as well as SMMs formed with their participation, are not among the most popular in the AHA family. This place is occupied primarily by the chain $\mathbf{C_2^2(6)}$**:**12/23 and the rings $\mathbf{R_2^2(10)}$**:**23/23 and $\mathbf{R_3^3(11)}$**:**12/23/23 (Scheme 7).

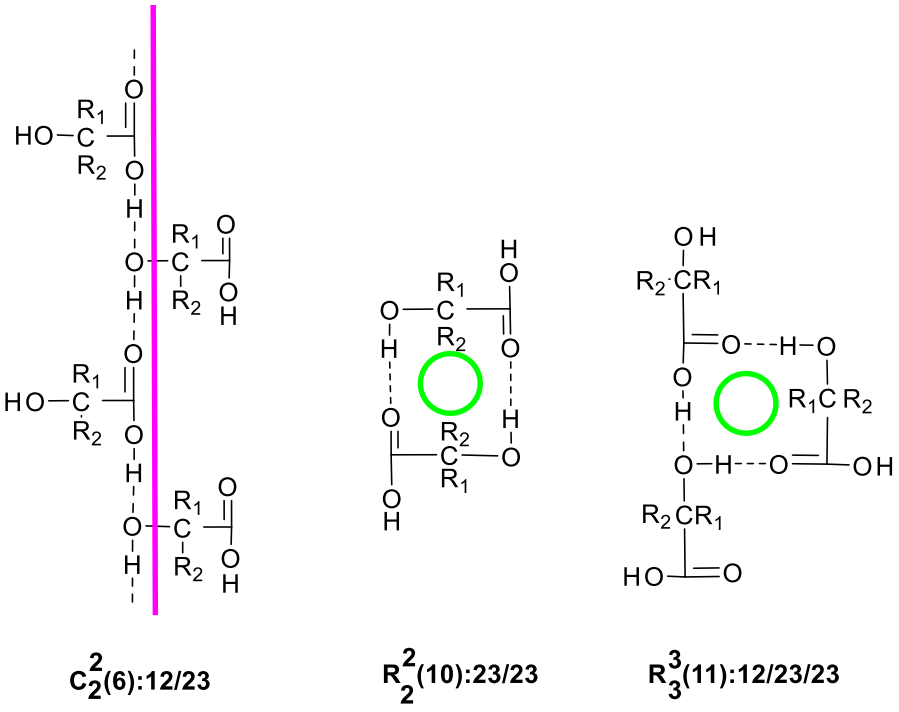

Scheme 7. Linear and cyclic synthons prevailing in crystals of α-hydroxycarboxylic acids.

Since linear synthons can form around open symmetry elements of both the first (screw axes) and the second kind (glide planes), they are less demanding on the symmetry of the crystal packing. On the contrary, cyclic synthons often form around the center of inversion and in this case can only be realized in an achiral or racemic environment. Of the two rings distinguished by frequency, the centrosymmetric ring $\mathbf{R_2^2(10)}$**:**23/23 belongs to such "chirality-dependent" synthons. On the contrary, the ring $\mathbf{R_3^3(11)}$**:**12/23/23, which is the second most common in the studied set, is not associated with central symmetry and, therefore, can be realized in a single-enantiomeric environment.

It is curious to note that in their good-quality study of the crystal organization of the representative set of mandelic acids, the authors of [41] drew attention to the synthon $\mathbf{R_2^2(10)}$**:**23/23 (denoting it as $\mathbf{R_2^2(10)}$), but synthon $\mathbf{R_3^3(11)}$**:**12/23/23 was not mentioned. It is clear that the reason for this was the specific nature of the sample, which consisted only of racemic compounds.

Previously, using examples of homogeneously organized sets of chiral compounds of different classes [10,11,42], we noted that cyclic synthons begin to dominate over linear

synthons upon passing from a single-enantiomeric to a racemic crystalline environment. In this work, we demonstrate that the chiral characteristics of the sample also play an important role in the choice of realizable cyclic synthons.

Supplementary Materials: The following supporting information can be downloaded at: https://www.mdpi.com/article/10.3390/cryst12101479/s1, Tables S1 and S2: Crystallographic summary of compounds *rac*-**1**–**4**, **6** (Table S1) and (*S*)-**1**–**5**, (*R*)-**6** (Table S2). Schemes S1–S18: Connectivity diagrams in crystals of the studied compounds.

Author Contributions: Conceptualization, writing—original draft preparation, writing—review and editing, A.A.B.; SC-XRD experiments of compounds *rac*-**1**–**4** and (*S*)-**1**–**5**, R.R.F.; SC-XRD experiments of compounds *rac*-**6** and (*R*)-**6**, A.T.G.; methodology, sample preparation, proofreading manuscript, Z.A.B. All authors have read and agreed to the published version of the manuscript.

Funding: This research received no external funding.

Institutional Review Board Statement: Not applicable.

Informed Consent Statement: Not applicable.

Data Availability Statement: Not applicable.

Acknowledgments: The authors are grateful to the Assigned Spectral-Analytical Center of FRC Kazan Scientific Center of RAS for technical assistance in research.

Conflicts of Interest: The authors declare no conflict of interest.

References

1. Price, S.L. Predicting crystal structures of organic compounds. *Chem. Soc. Rev.* **2014**, *43*, 2098–2111. [CrossRef] [PubMed]
2. Bowskill, D.H.; Sugden, I.J.; Konstantinopoulos, S.; Adjiman, C.S.; Pantelides, C.C. Crystal Structure Prediction Methods for Organic Molecules: State of the Art. *Annu. Rev. Chem. Biomol. Eng.* **2021**, *12*, 593–623. [CrossRef] [PubMed]
3. Thakur, T.S.; Dubey, R.; Desiraju, G.R. Crystal Structure and Prediction. *Annu. Rev. Phys. Chem.* **2015**, *66*, 21–42. [CrossRef] [PubMed]
4. Desiraju, G.R. Crystal Engineering: From Molecule to Crystal. *J. Am. Chem. Soc.* **2013**, *135*, 9952–9967. [CrossRef]
5. Corpinot, M.K.; Bučar, D.-K. A Practical Guide to the Design of Molecular Crystals. *Cryst. Growth Des.* **2019**, *19*, 1426–1453. [CrossRef]
6. Pasteur, L. Mémoire sur la relation qui peut exister entre la forme cristalline et la composition chimique, et sur la cause de la polarisation rotatoire. *C. R. Séances Acad. Sci.* **1848**, *26*, 535–538.
7. Pasteur, L. Recherches sur les relations qui peuvent exister entre la forme crystalline, la composition chimique et le sens de la polarisation rotatoire. *Ann. Chim. Phys.* **1848**, *24*, 442–459.
8. Wislicenus, J. Über die isomeren Milchsäure. *Ber. Dtsch. Chem. Ges.* **1869**, *2*, 619–621.
9. Wislicenus, J. Über die isomeren Milchsäure. 2. Abt. XXV. Über die optich-active Milchsäure der Fleischflüssigkeit. *Ann. Chem.* **1873**, *167*, 302–346. [CrossRef]
10. Bredikhin, A.A.; Bredikhina, Z.A.; Gubaidullin, A.T. Chirality-dependent supramolecular synthons based on the 1,3-oxazolidin-2-one framework: Chiral drugs mephenoxalone, metaxalone and 114 other examples. *CrystEngComm* **2020**, *22*, 7252–7261. [CrossRef]
11. Bredikhin, A.; Gubaidullin, A.; Bredikhina, Z.; Fayzullin, R.; Lodochnikova, O. Chirality, Gelation Ability and Crystal Structure: Together or Apart? Alkyl Phenyl Ethers of Glycerol as Simple LMWGs. *Symmetry* **2021**, *13*, 732. [CrossRef]
12. Bredikhina, Z.A.; Pashagin, A.V.; Kurenkov, A.V.; Bredikhin, A.A. Synthesis of enantiomerically pure 3-aryloxy-2-hydroxypropanoic acids, intermediate products in the synthesis of cis-4-Aminochroman-3-ols. *Russ. J. Org. Chem.* **2014**, *50*, 535–539. [CrossRef]
13. Kabsch, W. XDS. *Acta Crystallogr. Sect. D Biol. Crystallogr.* **2010**, *66*, 125–132. [CrossRef] [PubMed]
14. Sheldrick, G.M. *SHELXT*—Integrated space-group and crystal-structure determination. *Acta Crystallogr. Sect. A Found. Adv.* **2015**, *71*, 3–8. [CrossRef] [PubMed]
15. Sheldrick, G.M. Crystal structure refinement with *SHELXL*. *Acta Crystallogr. Sect. C Struct. Chem.* **2015**, *71*, 3–8. [CrossRef]
16. Etter, M.C. Encoding and decoding hydrogen-bond patterns of organic compounds. *Acc. Chem. Res.* **1990**, *23*, 120–126. [CrossRef]
17. Bernstein, J.; Davis, R.E.; Shimoni, L.; Chang, N.-L. Patterns in Hydrogen Bonding: Functionality and Graph Set Analysis in Crystals. *Angew. Chem. Int. Ed. Engl.* **1995**, *34*, 1555–1573. [CrossRef]
18. Desiraju, G.R. Designer crystals: Intermolecular interactions, network structures and supramolecular synthons. *Chem. Commun.* **1997**, 1475–1482. [CrossRef]
19. Betz, R.; Klüfers, P. 2,2-Dicyclopropylglycolic acid. *Acta Crystallogr. Sect. E Struct. Rep. Online* **2007**, *63*, o4921. [CrossRef]

20. Betz, R.; Klüfers, P. 1-Hydroxycyclopropane-1-carboxylic acid. *Acta Crystallogr. Sect. E Struct. Rep. Online* **2007**, *63*, o3891. [CrossRef]
21. Xu, L.-Z.; An, G.-W.; Yang, X.-D.; Yi, X. 1-Hydroxycyclohexanecarboxylic acid. *Acta Crystallogr. Sect. E Struct. Rep. Online* **2007**, *63*, o4213. [CrossRef]
22. Kanters, J.A.; Gaykema, W.P.J.; Roelofsen, G. Conformation and hydrogen bonding of disaccharides: The crystal and molecular structure of turanose [O-α-d-glucopyranosyl-(1→3)-β-d-fructopyranose] . *Cryst. Struct. Commun.* **1978**, *7*, 463.
23. Gerber, T.; Betz, R. 3,3,3-Trifluoro-2-hydroxy-2-(trifluoromethyl)propionic acid. *Acta Crystallogr. Sect. E Struct. Rep. Online* **2013**, *69*, o335. [CrossRef] [PubMed]
24. Rheingold, A.L. Private Communication to CCDC. 2019. Available online: https://www.ccdc.cam.ac.uk/support-and-resoureces/ccdcresouces (accessed on 15 May 2022).
25. Betz, R.; Klüfers, P. 1-Hydroxycyclobutane-1-carboxylic acid. *Acta Crystallogr. Sect. E Struct. Rep. Online* **2007**, *63*, o4032. [CrossRef]
26. Hosten, E.C.; Betz, R. Crystal structure of 2-ethyl-2-hydroxybutyric acid, at 200 K, C6H12O3. *Z. Kristallogr. New Cryst. Struct.* **2014**, *229*, 435–436. [CrossRef]
27. Pijper, W.P. The molecular and crystal structure of glycollic acid. *Acta Crystallogr. Sect. B Struct. Crystallogr. Cryst. Chem.* **1971**, *27*, 344–348. [CrossRef]
28. Ellison, R.D.; Johnson, C.K.; Levy, H.A. Glycolic acid: Direct neutron diffraction determination of crystal structure and thermal motion analysis. *Acta Crystallogr. Sect. B Struct. Crystallogr. Cryst. Chem.* **1971**, *27*, 333–344. [CrossRef]
29. Herbstein, F.H.; Kapon, M.; Reisner, G.M. syn-2-Hydroxy, 2-carboxyl[4.4.1]propellane-6-ene. *Z. Kristallogr.* **1998**, *213*, 551–558. [CrossRef]
30. Qiu, Y.; Wang, K.; Liu, Y.; Deng, H.; Sun, F.; Cai, Y. Synthesis, characterization and 1D helical chain crystal structure of [Cu(DBA)(2)(1,10-phen)](n) and [Cd(DBA)(2)(1,10-phen)(2)] (DBA = benzilic acid). *Inorg. Chim. Acta* **2007**, *360*, 1819. [CrossRef]
31. Betz, R.; Klüfers, P. 1-Hydroxycyclopentane-1-carboxylic acid. *Acta Crystallogr. Sect. E Struct. Rep. Online* **2007**, *63*, o3932. [CrossRef]
32. Oishi, M.; Kajiwara, M. Synthesis and Structural Features of a Lithium Borate Derived from 2,2-Dipropylglycolic Acid. *Bull. Chem. Soc. Jpn.* **2018**, *91*, 12–18. [CrossRef]
33. Gordon, M.N.; Liu, Y.; Shafei, I.H.; Brown, M.K.; Skrabalak, S.E. Crystal structures of three β-halolactic acids: Hydrogen bonding resulting in differing Z'. *Acta Crystallogr. Sect. C Struct. Chem.* **2022**, *78*, 257–264. [CrossRef] [PubMed]
34. Dahlén, B.; Lundén, B.-M.; Pascher, I. The crystal structure of 2-DL-hydroxytetradecanoic acid. *Acta Crystallogr. Sect. B Struct. Crystallogr. Cryst. Chem.* **1976**, *32*, 2059–2063. [CrossRef]
35. Navare, P.S.; MacDonald, J.C. Investigation of Stability and Structure in Three Homochiral and Heterochiral Crystalline Forms of 3-Phenyllactic Acid. *Cryst. Growth Des.* **2011**, *11*, 2422–2428. [CrossRef]
36. Tumanova, N.; Payen, R.; Springuel, G.; Norberg, B.; Robeyns, K.; Le Duff, C.; Wouters, J.; Leyssens, T. Cocrystallization out of the blue: Dl-mandelic acid/ethyl-dl-mandelate cocrystal. *J. Mol. Struct.* **2017**, *1127*, 397–402. [CrossRef]
37. Das, D.; Desiraju, G.R. Effects of the substituent on the formation of dimers and catemers in phenylpyruvic acids. *Cryst. Eng. Comm.* **2006**, *8*, 674–679. [CrossRef]
38. Wang, H.-Q.; Zeng, Q.-L.; Fang, H.; Huang, R.-B.; Zhao, Y.-F. (S)-3-[4-(Benzyloxy)phenyl]-2-hydroxypropanoic acid. *Acta Crystallogr. Sect. E Struct. Rep. Online* **2005**, *61*, o2286. [CrossRef]
39. Wang, Y.; van den Akker, N.M.S.V.D.; Molin, D.G.M.; Gagliardi, M.; van der Marel, C.; Lutz, M.; Knetsch, M.L.W.; Koole, L.H. A Nontoxic Additive to Introduce X-Ray Contrast into Poly(Lactic Acid). Implications for Transient Medical Implants Such as Bio-resorbable Coronary Vascular Scaffolds. *Adv. Healthc. Materials.* **2014**, *3*, 290–299. [CrossRef]
40. Schouten, A.; Kanters, J.A.; van Krieken, J. Low temperature crystal structure and molecular conformation of l-(+)-lactic acid. *J. Mol. Struct.* **1994**, *323*, 165–168. [CrossRef]
41. Coles, S.J.; Ellis, A.L.; Leung, K.; Sarson, J.; Threlfall, T.L.; Tizzard, G.J. Relationships between the racemic structures of substituted mandelic acids containing 8- and 10-membered hydrogen bonded dimer rings. *CrystEngComm* **2014**, *16*, 10816–10823. [CrossRef]
42. Bredikhin, A.A.; Fayzullin, R.R.; Bredikhina, Z.A. Crystal Structure of Chiral Drug Prenalterol and Its Precursor Prone to Spontaneous Resolution. *Symmetry* **2022**, *14*, 1150. [CrossRef]